ADVANCED FUNCTIONAL MATERIALS

Charge-Transport Behavior in Aligned Carbon Nanotubes: A Quantum-Chemical Investigation**

By *Xia Yang*, *Liping Chen*, *Zhigang Shuai*,* *Yunqi Liu*, and *Daoben Zhu*

Correlated quantum-chemical calculations are applied to analyze the amplitude of the electronic-transfer integrals that describe charge transport in interacting carbon nanotubes (CNTs) by investigating the influences of: i) the relative positions of the CNTs, ii) the size of the CNTs, and iii) their chemical impurities. Our results indicate that the mobility of the charge carrier is extremely sensitive to the molecular packing and the presence of chemical impurities. The largest splitting for the highest occupied molecular orbital (HOMO) and lowest unoccupied molecular orbital (LUMO) levels is in the case of perfectly cofacial conformations where hexagons face hexagons in the dimer structure. We found that the diameter of the CNT determines the type of transporting carrier: for CNTs with large diameters hole transport dominates, while for thin CNTs electron transport dominates. In general, the carrier mobility for the perfect CNTs ($n \geq 3$) is less pronounced than that of C_{60} due to their relatively small strain. B- and N-doped CNTs exhibit considerably larger mobilities owing to the possibility of metallic behavior. These results provide a plausible explanation for the high mobility found experimentally in a field-effect transistor (FET) made from a large-area, well-aligned CNT array. In addition, these hole-rich and electron-rich dopants imply potential applications in nanoelectronics.

1. Introduction

In recent years, nanomaterials, molecular and polymeric materials, and biomaterials have been found to possess great potential in nanoscale electronics.[1–3] Charge-transport behavior in these materials is the key issue to address both experimentally and theoretically. Difficulties have been encountered in understanding the transport behaviors in active conjugated-polymer films[4] and in proteins.[5,6]

Among the promising candidates as building blocks for molecular-scale materials, carbon nanotubes (CNTs) and doped nanotubes offer remarkable potential as active elements in nanosized electronic and photonic devices, such as CNT field-effect transistors (CNTFETs),[7–9] high-current-carrying capabilities,[10] and logical circuits based on individual carbon nanotubes.[11,12] In particular, two-dimensional (2D) aligned carbon nanotube films exhibit highly anisotropic physical and chemical properties that have received increasing attention for their application in nanodevices.[13,14] Such devices are expected to be integrated, for instance, into large arrays that show an ON/OFF switching operation. Moreover, for high-temperature applications, nanotube films would be superior to organic films in performance and reliability due to the less significant degradation in nanotube structural properties at high temperatures. In all of these applications, control of carrier mobility is a basic requirement for the design of efficient electronic devices, because the performance of these devices depends largely on the efficiency of the charge-transport processes.

Previous investigations[15–17] have shown that the charge-transport properties depend critically on the degree of ordering of the chains in the solid state as well as on the density of chemical or structural defects, which explains why the experimental characterization of transport properties in thin films or crystals has led to results that vary with sample quality. Recently, thin-film transistors based on aligned carbon nanotubes have been fabricated by Xiao et al.;[18] they demonstrated an extremely high charge mobility of about 61.6 $cm^2 V^{-1} s^{-1}$, similar to heavily doped n-Si.[19] However, the mechanism of the tube–tube interaction of aligned nanotube films in field-effect transistor (FET) behavior is unclear. It is therefore of the utmost interest to understand the underlying mechanism for such a high mobility.

One of the major parameters governing the transport properties at the microscopic level is the amplitude of the electronic transfer integrals between "sites", for example in a Buttiker–Landauer[20–22] expression for conductivity[23,24] or in the Marcus formulation[5] for electron transfer. Cornil et al. have developed a semi-empirical INDO (intermediate neglect of differential overlap) method which can be used to obtain good estimates of the transfer integrals in van der Waals bonded molecules.[25–27] The inter-tube transfer integral, t, which reflects the whole band curvature, expresses the ease of transfer of a charge between two interacting tubes. It can thus be used to tailor the transport properties of CNT-based thin films. Here we exploit a semi-empirical quantum-chemical approach to characterize the key parameters governing charge transport in CNTs made of carbon nanotube molecules and their derivatives, and seek to establish structure–property relationships by

[*] Prof. Z.-G. Shuai, Dr. X. Yang, L.-P. Chen, Prof. Y.-Q. Liu, Prof. D.-B. Zhu
Laboratory of Organic Solids, Center for Molecular Sciences
Institute of Chemistry, Chinese Academy of Sciences
Beijing 100080 (P.R. China)
E-mail: zgshuai@iccas.ac.cn

[**] This work was supported by the National Science Foundation of China, the "973 program" from the Ministry of Science and Technology of China, and the Chinese Academy of Sciences.

 DOI: 10.1002/adfm.200304481

analyzing how these integrals are affected at the molecular scale by the nature, size, and relative position of the interacting units, which could serve as a framework to interpret the experimental results.

1.1. Theoretical Methodology

In the case of a cofacial dimer built from two CNT chains and separated by an intermolecular distance, d, the total Hamiltonian for such a dimer is

$$H_{tot} = H_1 + H_2 + H_{12} \quad (1)$$

with H_1 (H_2) the Hamiltonian for the isolated tube 1 (2) and H_{12} the term representing the inter-tube interactions. For two identical CNT chains

$$|\Psi^{\pm}\rangle = (1/\sqrt{2})(|\Psi_1^*\rangle|\Psi_2\rangle \pm |\Psi_1\rangle|\Psi_2^*\rangle) \quad (2)$$

where $|\Psi_n\rangle$ and $|\Psi_n^*\rangle$ denote the wavefunctions for the ground state and the ionized state, respectively, and ± corresponds to the symmetric/antisymmetric combination of the equivalent $|\Psi_1^*\rangle|\Psi_2\rangle$ and $|\Psi_1\rangle|\Psi_2^*\rangle$ wavefunctions. The molecular geometries for isolated CNTs of different sizes and forms were optimized by means of the semi-empirical AM1 (Austin Model 1) method[28] and the electronic structures for the isolated molecule and the supramolecular systems were calculated with the semi-empirical INDO Hamiltonian (as developed by Zerner and coworkers for spectroscopic purposes[25,29]). In the case of a symmetric dimer, the energy splitting described by Equation 2 is given to the first order by[30]

$$W = \langle\Psi^+|H_{tot}|\Psi^+\rangle - \langle\Psi^-|H_{tot}|\Psi^-\rangle = 2\langle\Psi_1^*\Psi_2|H_{12}|\Psi_1\Psi_2^*\rangle = 2|t| \quad (3)$$

This expression can be easily generalized to the bandwidth of a one-dimensional crystal when only nearest-neighbor interactions are retained: $W = 4|t|$ in this case.[30] In the framework of tight-binding models, the total bandwidth for a one-dimensional stack is expressed as $4t \times \cos[\pi/(n+1)]$, with n being the number of molecules in the stack; by extension, the total bandwidth can be expressed for any molecular packing from the amplitude of the transfer integral t between the various interacting units. For simple cosine-shaped bands, the higher the HOMO (LUMO) bandwidth, the higher the expected hole (electron) mobility (HOMO = highest occupied molecular orbital; LUMO = lowest unoccupied molecular orbital.

At the microscopic level, the charge-transport mechanism can then be described as involving an electron transfer from a charged molecule to an adjacent neutral molecule. According to the semi-classical Marcus theory,[31] the electron-transfer (hopping) rate k_{et} can be estimated to a good approximation as

$$k_{et} = (4\pi^2/h)t^2(4\pi\lambda k_B T)^{-0.5} \exp(-\lambda/4k_B T) \quad (4)$$

where h and k_B are the Planck and Boltzmann constants, respectively. The reorganization energy, λ, describing the strength of the electron–phonon vibration, can be reliably estimated as twice the relaxation energy of a polaron localized over a single unit when neglecting the change in polarization of the surrounding medium during the hopping event; t corresponds to the inter-tube transfer integral that describes the strength of the interaction between adjacent CNTs. It should be noted that the presence of t in Equation 4 applies to situations where the charge transfer between the initial and final states involved in the hopping process can be described by a simple consideration of the molecular-orbital levels, i.e., a one-electron approach—the many-body wavefunction can be represented by the frontier orbitals within the scope of Koopmans' theorem. The transfer integral associated with a given electronic level is related to the energetic splitting of that level when going from an isolated molecule to the dimer. Thus, hole (electron) transport can be estimated by a transfer integral that corresponds to half of the splitting of the HOMO (LUMO) level. The calculated t value is rationalized by means of an analysis of the shape of the frontier orbitals of the isolated tubes and the bonding-antibonding overlap pattern of the HOMO and LUMO wavefunctions determined by the relative positions of the interacting tubes in the dimers (visualized by means of the ZOA v.2.0 program[32]). This methodology has been successfully applied to study different model systems, including different diameter, length and B,N-doped CNTs to evaluate the influence on the transfer integral values.

2. Results and Discussion

A series of armchair (n,n) single-walled carbon nanotubes (SWCNTs; $n = 2$–9) consisting of different carbon layers were used as model systems. The dangling bonds at the ends of the tubes were saturated with H atoms. We considered perfectly cofacial dimers made of two CNTs molecules in which the hexagons of one CNT are exactly superimposed on top of those of the other one. The interaction between the two aligned tubes leads to a splitting of the HOMO/LUMO level, which is either fully bonding, leading to a very stabilized level (e.g. the dimer H–1/L), or fully antibonding, leading to a very destabilized level (e.g., the dimer H/L+1), as illustrated in Figure 1.

2.1. Influence of CNT Relative Positions

In many instances, cofacial packing affects the relative positions of adjacent molecules. Here we have chosen (5,5) SWCNT as our model system for some basic operations such as separation, translation and rotation. Figure 2 describes the evolution of the transfer integrals between the frontier electronic levels in a perfect hexagon-to-hexagon dimer formed by two eight-layered (5,5) models, as a function of the intermolecular separation between 3.0 and 6.0 Å. The HOMO splittings are calculated to be slightly larger than the LUMO splittings whatever the inter-tube separation. This suggests that a hole is more mobile than electrons in well-ordered one-dimensional stacks. The magnitude of the splitting is found to decay expo-

ADVANCED FUNCTIONAL MATERIALS

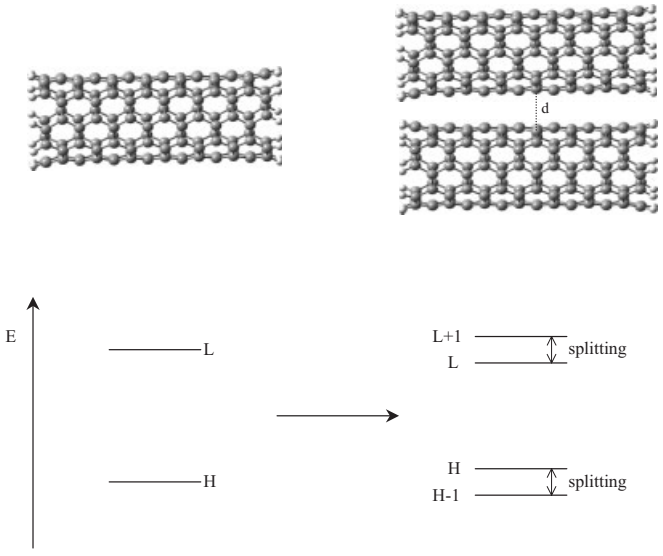

Figure 1. Schematic representation of the one-electron structure of a single nanotube and that of a cofacial dimer formed by two tubes with a separation distance *d*. The ZINDO-calculated energy splittings of the HOMO and LUMO levels when going from the isolated nanotube molecule to the dimer are also shown.

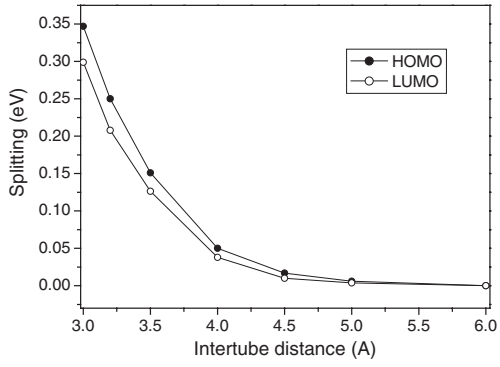

Figure 2. ZINDO-calculated splitting of the HOMO and LUMO levels in dimers as a function of the inter-tube distance.

nentially with the inter-tube distance, which mainly results from the exponential decay in intermolecular overlap of the π atomic orbital when the two molecules are pulled apart.

The overlap of the molecular orbitals is made up of the sum of many atomic overlaps with a product of linear combination of atomic orbitals (LCAO) coefficients. The more nodal surfaces, the more cancellation of terms is possible due to the signs of the products of the coefficients. Hence, a simple way to rationalize the fact that the HOMO levels have a larger overlap than the LUMO levels for the (5,5) CNT dimer is that there are more nodal surfaces in the LUMO wavefunction than in the HOMO.

We then performed a translation operation in which one tube is translated along its longitudinal axis while keeping the planes of the units parallel, with the inter-tube distance fixed at 3.5 Å (which is close to the interlayer distance in graphite). The result, illustrated in Figure 3, shows a clear oscillatory

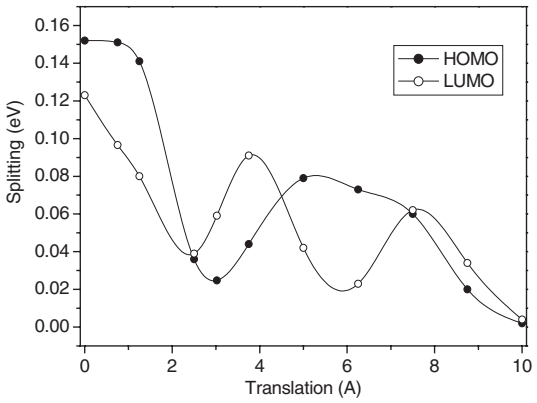

Figure 3. ZINDO-calculated electronic splittings of the HOMO and LUMO levels in a dimer formed by two molecules separated by 3.5 Å as a function of the degree of translation of one molecule along its long tube-axis.

nature, with a general trend of decreasing splitting with increasing translational shifts, indicating that glided molecules introduce a significant resistance to charge transport along the tube axes. The magnitude of the splitting decreases progressively as the spatial overlap between the wavefunctions of the two neighboring tubes is decreased. The local maxima in the course of the translation are dominated by a high degree of bonding or antibonding overlap between the six-membered rings of the two CNTs.

In addition to the perfectly cofacial dimer situation, we also investigated the impact of rotational disorder on the transport properties by rotating one molecule in the stacking plane around its long tube-axis (with the inter-tube distance fixed at 3.5 Å), thus breaking the face-to-face ordering of the hexagons of the two units. The calculated splittings illustrated in Figure 4 display strong oscillations as a function of the rotational angle between the two CNTs. The carrier mobilities are expected to be maxima in the cofacial conformations. The HOMO and LUMO splittings show a synchronous periodicity at a regular angle of 72° as a result of the D_{5d} symmetry of the (5,5) tube.

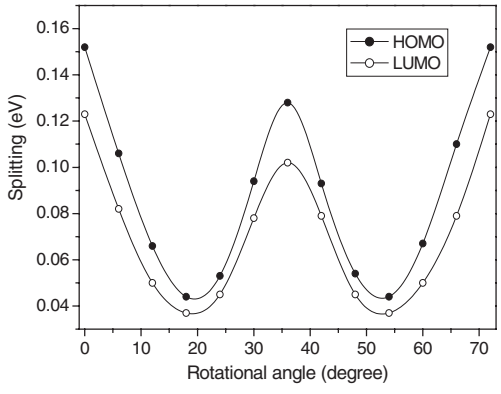

Figure 4. ZINDO-calculated evolution of the HOMO and LUMO splittings in a dimer (inter-tube distance fixed at 3.5 Å) as a function of the rotation of one molecule around the long tube-axis. (The range between 0 and 72° is spanned, the rest of the data are the same due to the D_{5d} symmetry of the (5,5) tube.)

A dramatic change for a small rotational disorder is associated with the extent of overlap between the wavefunctions of the two molecules. The large splitting at 36° in an oscillation period is dominated by full bonding or antibonding interactions between the π-atomic orbitals localized in geometries where the carbon–carbon double bonds of one tube are superimposed over the center of the six-membered rings of the other tube. In contrast, the minima—the HOMO splittings decreasing to about 0.05 eV and the LUMO splittings down to even less—are observed for such configurations where the carbon atoms of one molecule are superimposed over the center of the hexagons of the other molecule, thus reducing the global overlap considerably.

2.2. Influence of CNT Size

We then investigated the evolution of the splitting of the HOMO and LUMO levels as a function of the CNT sizes, including length and diameter. Figure 5 shows the evolution of the transfer integrals, calculated at the ZINDO (Zerner' intermediate neglect of differential overlap) level, between the frontier electronic levels in perfect hexagon-to-hexagon dimers

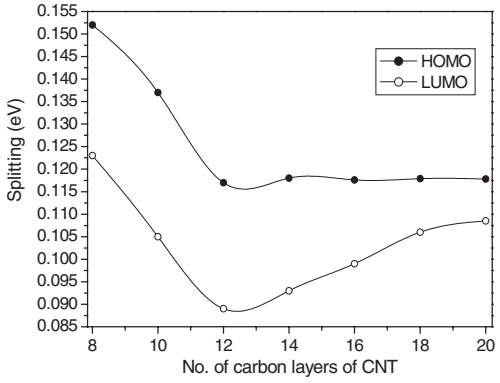

Figure 5. ZINDO-calculated evolution of the HOMO and LUMO splittings in dimers formed by two hexagon-to-hexagon nanotubes (with a fixed distance of 3.5 Å) as a function of the number of carbon layers of the CNT.

formed by two (5,5) SWCNTs with a separation of 3.5 Å as a function of the nanotube length. We found that the HOMO and LUMO splittings begin to decrease with the tube length, then the HOMO splittings tend to saturate, while the LUMO splittings slightly increase until they saturate at a value lower than that for the HOMO splittings. This indicates that hole mobility can be favored over electron mobility for (5,5) armchair CNTs.

This result can be rationalized by the fact that, according to a qualitative rule, the lower the number of nodes in the wavefunction of a given frontier level of an isolated molecule, the larger the splitting of that level in the case of a perfectly cofacial dimer. From eight layers to twelve layers, the HOMO and LUMO splittings decrease because of the appearance of an increasing number of antibonding interactions between two molecules in the dimer. When the tube length increases to more than twelve layers, the bonding–antibonding character of the electronic interaction at the LUMO level begins to strengthen, which contributes to an increase of the LUMO splitting. The relative difference in the number of nodes at the HOMO and LUMO levels becomes less and less as the tube length continues to increase, hence the HOMO and LUMO splittings also work up to the saturated value.

The evolutions of the HOMO and LUMO splittings for CNT dimers with a tube diameter going from $n = 2$ to $n = 9$ are given in Figure 6 (inter-tube distance fixed here at 3.5 Å). It can be seen that the computed HOMO and LUMO splittings decrease with increasing diameter for $n \geq 3$, and converge to a value of about 0.12 eV for tubes with large diameters ($n \geq 6$). It is most interesting to note that there are three distinct regions: i) for

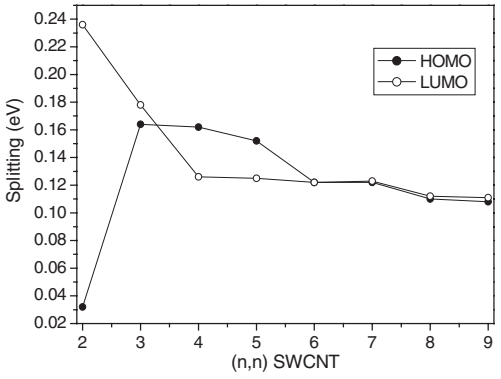

Figure 6. ZINDO-calculated electronic splittings of the HOMO and LUMO levels in dimers made of two nanotubes (with a fixed distance of 3.5 Å) as a function of the tube diameters.

the thin tubes, the electron transport dominates the hole transport ($n = 2,3$), i.e., the LUMO splitting is larger than that of the HOMO, ii) the hole transport dominates the electron transport for $n = 4,5$, namely, the HOMO splitting is larger than the LUMO splitting, and iii) the carrier transport is ambipolar for $n \geq 6$ because the HOMO and LUMO splittings are the same. Thus, by controlling the diameter of the CNT, the transport behaviors can be tailored.

For the sake of comparison, the relatively large splitting for the different (n,n) tubes is listed in Table 1, along with the pyramidalization angle, θ_p, which is defined as the angle between

Table 1. Pyramidalization angle θ_p [°] and relative large splitting [eV] for (n,n) CNTs with different diameters [Å].

(n,n) CNT	(2,2)	C_{60} [b]	(3,3)	(4,4)	(5,5)	(6,6)	(7,7)	(8,8)	(9,9)
Diameter [Å]	2.75	7.10	4.12	5.50	6.87	8.25	9.62	11.00	12.37
θ_p [a]	13.96	11.64	11.50	7.95	5.97	4.99	4.27	3.74	3.33
Relative large splitting [eV]	0.24 (L)	0.21 (H)	0.18 (L)	0.16 (H)	0.15 (H)	0.12 (H=L)	0.12 (H=L)	0.11 (H=L)	0.11 (H=L)

[a] The pyramidalization angles θ_p are defined by the angle between the π-orbital and adjacent σ-bonds, which were determined by π-orbital axis vector (POAV) analysis [33,34]. [b] The ZINDO-calculated LUMO splitting of C_{60} is 0.082 eV.

ADVANCED FUNCTIONAL MATERIALS

the π-orbital and adjacent σ-bonds, which can be determined by a π-orbital axis vector (POAV) analysis.[33,34] The pyramidalization angle, θ_p, is used to characterize the strain. It can be seen that the larger the strain in the CNT, the greater the carrier mobility. One can also note that (*n*,*n*) CNTs in general possess a lower mobility than that of C_{60}. In addition, the hole transport in C_{60}, with a diameter close to that of a (5,5) tube, is more favorable, in contrast to the highly pyramidalized CNTs—the (2,2) and (3,3) tubes. These suggest the strain is likely to be the major driving force for mobility, while the diameter plays an important role in determining the transport type, hole or electron.

From the above examination of the transport properties of CNTs, it can be further understood that the splittings of the frontier electronic levels in a dimer are directly related to both the spatial overlap and the nature of the electronic wavefunctions' interaction. The stronger the bonding character of the electronic interaction in the dimer, the stronger the antibonding character of the interaction for the dimer, and the larger the splitting. These are in agreement with the theoretical investigations on π-conjugated oligomers and polymers previously made by Brédas, Cornil, and co-workers.[35,36]

2.3. Influence of Chemical Impurities

Modifications of the electronic structure due to the introduction of boron and nitrogen into the CNT have been studied by scanning tunneling spectroscopy.[37,38] To obtain a better understanding of the carrier-transport properties of well-aligned doped CNTs, we investigated the effects of an impurity by introducing one and three boron or nitrogen atoms into an eight-layered metallic (5,5) carbon nanotube. The dopant atoms were located at the tube's center for individual substitution and at the straight sections of the nanotubes along the wall, resulting in a bamboo-like structure, for triple substitutions. Table 2 presents a range of HOMO and LUMO splittings due to B- and N-atom substitution, which were obtained by performing the same rotational operation as the above undoped CNTs. It is clearly seen that the HOMO splittings of the incorporation of B-atoms within a single CNT, or the LUMO splittings of the embedding of pyridine-like N units within a single CNT, are one order of magnitude larger than that of pure CNT, which indicates that the hole and electron mobilities are strongly influenced by the introduction of B- and N-atoms into the carbon lattice. This is consistent with the fact that B- and N-doping correspond to acceptor states (p-type doping) and donor states (n-type doping), respectively. Such large mobilities for the doped CNTs can be ascribed to the half-filled band (formed by the singly occupied MO of doped CNT, if packed regularly) that is responsible for metallic behavior.

Table 2. The HOMO and LUMO splittings [eV] for pure CNTs and the range of the HOMO and LUMO splittings for doped CNTs obtained by rotating one molecule in the stacking plane around its long tube-axis from 0° to 360°.

	Pure (5,5) CNT	B-doped CNT		N-doped CNT	
		1B	3B	1N	3N
HOMO splitting	0.152	2.280–2.308	2.300–2.543	0.150–0.157	0.100–0.326
LUMO splitting	0.125	0.123–0.130	0.120–0.466	2.228–2.300	1.580–2.302

We also investigated the rotation-dependence of the splitting for the doped CNTs. No oscillation similar to Figure 4 is found when one molecule is rotated around the tube axis from 0° (N atoms to N atoms in cofacial hexagons of the two units) to 360°. The main reason is that the HOMO and LUMO orbitals are largely localized near the dopant atoms instead of being symmetrically distributed in a manner similar to the perfect CNT. The splittings of the HOMO and LUMO thereby exhibit a decrease with increasing separation between the N atoms of the two molecules owing to the decrease of the orbital overlap.

At the same time, we investigated the effect of a pair of B- or N-atoms at different substitution positions on the transfer integral. For a pair of B- or N-doped (5,5) nanotubes, the splittings range from 0.060 eV to 0.180 eV for the HOMO splitting and from 0.016 eV to 0.124 eV for the LUMO splitting, suggesting that mobility is similar or even lower than that of the pure (5,5) CNT (0.152 eV for the HOMO splitting and 0.125 eV for the LUMO splitting). This large difference in the splittings from the above single and triplet dopants can be rationalized by a change in the electronic structure of the single tube (illustrated in Fig. 7).

From Figure 7 it is clear that the electronic structures of these doped nanotubes are strongly modified by including electron-donor or -acceptor states near the conduction- or valence-band edge. The introduction of an odd number of N atoms into a carbon framework provides an additional electron at the SOMO (singly occupied MO) level whose energy is closer to that of the LUMO level than to the HOMO-1 level due to the electron-rich character of an N atom. It is thus easier to excite this additional electron to the LUMO than from the completely filled levels to the SOMO level, consequently providing an electron carrier for the conduction band (n-type conduction). In contrast, odd-numbered B-doping of a SWCNT provides an additional electron in the SOMO level close to the HOMO-1 level instead of the LUMO level on account of the electron deficiency of the B atom, which creates a hole-carrier in the valence band (p-type conduction). In the case of an even number of dopants, electron excitation from the occupied orbitals to the unoccupied orbitals requires a relatively large energy in comparison with CNTs containing an odd number of B or N atoms. An increase in the number of defects is likely to reduce the mean-free path of the electrons, thus resulting in a somewhat increased resistance for transport, i.e., relatively small splittings.

Therefore, such hole-rich and electron-rich dopants can be used to modify the majority carrier conduction from p-type to n-type, which could again pave the way to realize molecular heterojunction devices. These doped CNTs will show large mobilities, although the ON/OFF current ratio of these thin-film transistors (TFTs) is likely to decrease to a great extent due to

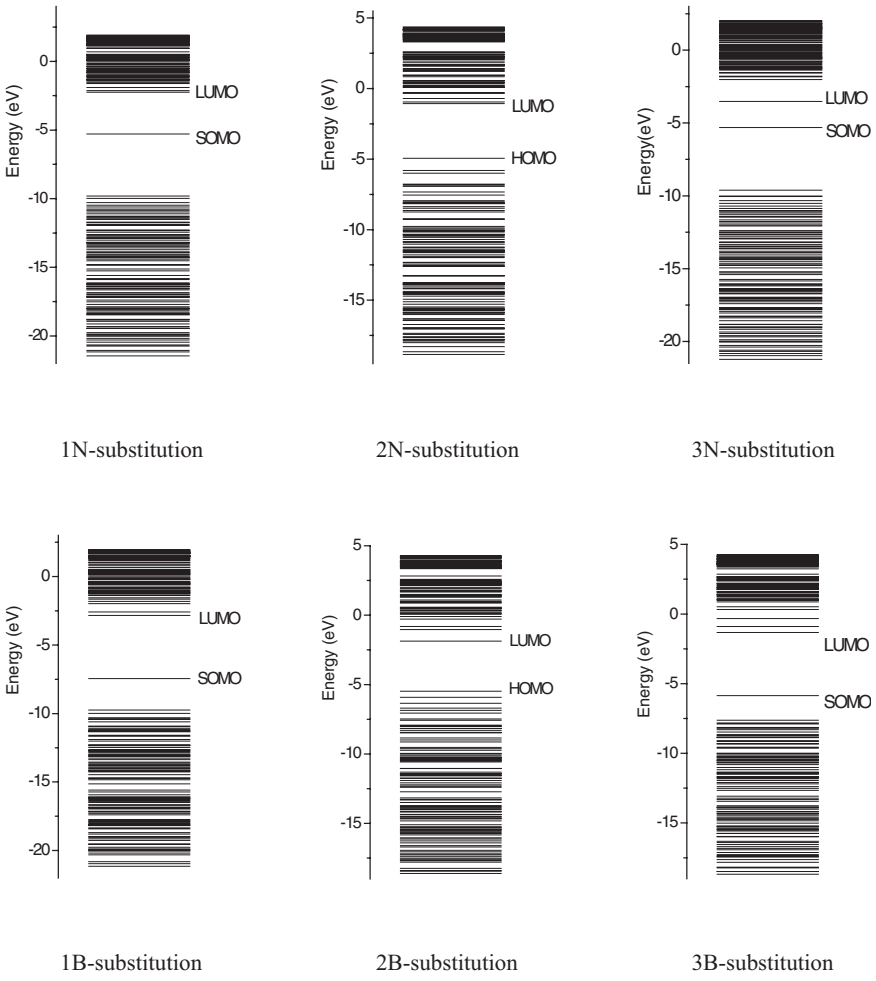

Figure 7. Schematic illustration of the energy levels of CNTs doped with one, two, and three B and N atoms.

the increasingly metallic behavior of the nanotube film. Thus, we can conclude that the low ON/OFF current ratio (about 64) of the TFTs with a very high mobility (ca. 61.6 $cm^2 V^{-1} s^{-1}$) in the experiment of Xiao et al.[18] is probably caused by a dopant such as pyridine-like N units.

3. Conclusion

In this work, we have performed correlated quantum-chemical calculations to illustrate, at the molecular level, how the amplitude of the transfer integrals that govern charge transport is highly sensitive to various aspects of nanotube molecular packing. The largest splittings for the HOMO and LUMO levels are found in perfectly cofacial configurations in which the hexagons of one of the tubes face the hexagons of another tube. In this case, electron mobility is found to be larger than the hole for small tubes ($n = 2,3$); the situation is opposite for $n = 4,5$. For $n \geq 6$, the splitting difference for the HOMO and LUMO levels is very small. We believe that the strain is likely to be the major driving force for mobility, while the diameter plays an important role in determining the transport type (hole or electron). It is expected that the transport behaviors can be tailored by controlling the diameter of the CNT.

Our results show that the mobility of the charge carriers in pure (n,n) CNTs ($n \geq 3$) could be less pronounced than that of a well-ordered C_{60} crystal. However, B- or N-doping of carbon nanotubes can cause a considerably larger mobility due to their possibly metallic behavior. This provides a plausible explanation for the behavior of the high-mobility TFTs based on a large-area, well-aligned carbon nanotube array with a relatively low ON/OFF current ratio in a previous study.[18]

At the same time, this novel doping scheme supplies us with a road map for the insertion of other electron rich or defect impurities into the carbon lattice for the creation of donor or acceptor states, and may well suggest a way to achieve full p–n junctions in carbon nanotubes.

Received: July 23, 2003
Final version: October 14, 2003

[1] S. P. Gubin, Y. V. Gulayev, G. B. Khomutov, V. V. Kislov, V. V. Kolesov, E. S. Soldatov, K. S. Sulaimankulov, A. S. Trifonov, *Nanotechnology* **2002**, *13*, 185.
[2] C. Videlot, J. Ackermann, P. Blanchard, J. M. Raimundo, P. Frere, M. Allain, R. de Bettignies, E. Levillain, J. Roncali, *Adv. Mater.* **2003**, *15*, 306.
[3] D. Pum, A. Neubauer, E. Gyorvary, M. Sara, U. B. Sleytr, *Nanotechnology* **2000**, *11*, 100.
[4] J. H. Burroughes, D. D. C. Bradley, A. R. Brown, R. N. Marks, K. Mackay, R. H. Friend, A. R. Burns, A. B. Holmes, *Nature* **1990**, *347*, 539.
[5] R. A. Marcus, N. Sutin, *Biochim. Biophys. Acta* **1985**, *811*, 265.
[6] V. S. Pande, J. N. Onuchic, *Phys. Rev. Lett.* **1997**, *78*, 146.
[7] S. Tans, A. Verschueren, C. Dekker, *Nature* **1998**, *393*, 49.
[8] R. Martel, T. Schmidt, H. R. Shea, T. Hertel, P. Avouris, *Appl. Phys. Lett.* **1998**, *73*, 2447.
[9] W. B. Choi, D. S. Chung, J. H. Kang, H. Y. Kim, Y. W. Jin, I. T. Han, Y. H. Lee, J. E. Jung, N. S. Lee, G.. S. Park, J. M. Kim, *Appl. Phys. Lett.* **1999**, *75*, 3129.
[10] S. Frank, P. Poncharal, Z. L. Wang, W. A. De Heer, *Science* **1998**, *280*, 1744.
[11] S. J. Wind, J. Appenzeller, R. Martel, V. Derycke, P. Avouris, *Appl. Phys. Lett.* **2002**, *80*, 3817.
[12] X. L. Liu, C. L. Lee, C. W. Zhou, J. Han, *Appl. Phys. Lett.* **2001**, *79*, 3329.
[13] P. G. Collins, A. Zettle, *Phys. Rev. B* **1997**, *55*, 9391.
[14] Y. Chen, D. T. Shaw, L. Guo, *Appl. Phys. Lett.* **2000**, *76*, 2469.
[15] J. G. Laquindanum, H. E. Katz, A. J. Lovinger, A. Dodabalapur, *Chem. Mater.* **1996**, *8*, 2542.
[16] D. J. Gundlach, Y. Y. Lin, T. N. Jackson, S. F. Nelson, D. G. Schlom, *IEEE Electron. Device Lett.* **1997**, *18*, 87.
[17] D. Fichou, *J. Mater. Chem.* **2000**, *10*, 571.
[18] K. Xiao, Y. Liu, P. Hu, G. Yu, X. Wang, D. Zhu, *Appl. Phys. Lett.* **2003**, *83*, 150.
[19] S. Takagi, M. Lwase, A. Torium, *Tech. Dig.—Int. Electron Devices Meet.* **1988**, 393.
[20] R. Landauer, *Philos. Mag.* **1970**, *21*, 863.
[21] M. Büttiker, Y. Imry, R. Landauer, S. Pinhas, *Phys. Rev. B* **1985**, *31*, 6207.
[22] M. Büttiker, *Phys. Rev. Lett.* **1986**, *57*, 1761.
[23] P. A. Schulz, D. S. Galvao, M. J. Caldas, *Phys. Rev. B* **1991**, *44*, 6073.
[24] R. Hey, F. Gagel, M. Schreiber, K. Maschke, *Phys. Rev. B* **1997**, *55*, 4231.
[25] J. Ridley, M. C. Zerner, *Theor. Chim. Acta* **1973**, *32*, 111.
[26] J. Cornil, J.-P. Calbert, D. Beljonne, R. Silbey, J.-L. Brédas, *Adv. Mater.* **2000**, *12*, 978.
[27] J. Cornil, J.-P. Calbert, J.-L. Brédas, *J. Am. Chem. Soc.* **2001**, *123*, 1250.
[28] M. J. S. Dewar, E. G. Zoebisch, E. F. Healy, J. J. P. Stewart, *J. Am. Chem. Soc.* **1985**, *107*, 3902.
[29] M. C. Zerner, G. H. Loew, R. F. Kichner, U. T. Mueller-Westerhoff, *J. Am. Chem. Soc.* **1980**, *102*, 589.
[30] M. Pope, C. E. Swenberg, *Electronic Processes in Organic Crystals*, Oxford University Press, New York **1982**.
[31] R. A. Marcus, *Rev. Mod. Phys.* **1993**, *65*, 599.
[32] J.-P. Calbert, ZOA V.2.0 software, see http://zoa.freeservers.com
[33] R. C. Haddon, *J. Phys. Chem. A* **2001**, *105*, 4164.
[34] R. C. Haddon, *Science* **1993**, *261*, 1545.
[35] J.-L. Brédas, J.-P. Calbert, D. A. da Silva Filho, J. Cornil, *Proc. Natl. Acad. Sci. USA* **2002**, *99*, 5804.
[36] J. Cornil, V. Lemaur, J.-P. Calbert, J.-L. Brédas, *Adv. Mater.* **2002**, *14*, 726.
[37] R. Czerw, M. Terrones, J.-C. Charlier, X. Blase, B. Foley, R. Kamalakaran, N. Grobert, H. Terrones, P. M. Ajayan, W. Blau, D. Tekleab, M. Rühle, D. L. Carroll, *Nano Lett.* **2001**, *1*, 457.
[38] D. L. Carroll, Ph. Redlich, X. Blase, J.-C. Charlier, S. Curran, P. M. Ajayan, S. Roth, M. Rühle, *Phys. Rev. Lett.* **1998**, *81*, 2332.

